Supporting Information

The self-assembly of polyacrylic acid nanoparticles induced by non-covalent interactions enhances the response of molecular fluorescence probes to formaldehyde

Qingxin Han[,#,a], Ruyun Sun[#,a], Xuechuan Wang[c], Lulu Ning[a], Luming Chen[a], Xiaoling Ling[b], Xiaoyu Guan[*,c]*

[a]*College of Bioresources Chemistry and Materials Engineering, Shaanxi University of Science and Technology, Xi'an 710021, P.R. China.*

[b]*College of Chemistry and Chemical Engineering, Shaanxi University of Science and Technology, Xi'an, 710021, China.*

[c]*Institute of Biomass & Functional Materials, Shaanxi University of Science and Technology, Xi'an 710021, P.R. China.*

*Corresponding author: hanqingxin@sust.edu.cn; guanxiaoyu@sust.edu.cn.

[#]*These authors contributed equally to this work and should be regarded as co-first authors.*

Table of Contents

1. Experimental Section Supplement

Synthesis of probe MBNI

Compound NBBN was also utilized in the synthesis of MBNI. In brief, NBBN (5.4 g, 16.3 mmol), CH_3ONa (7.0 g, 130 mmol), and $CuSO_4 \cdot 5H_2O$ (0.50 g, 2.0 mmol) were refluxed in 50 mL of methanol for 12 hours. Following solvent evaporation, the residue underwent triple washing with water and subsequent vacuum drying. The crude product was purified by silica gel column chromatography (ethyl acetate/petroleum ether = 1:15, v/v), yielding the final white powdery MBNI product.

Spectral response study of PAA@NBHN towards FA

In the polymer screening experiment, the fluorescence response of NBHN to formaldehyde was evaluated using fluorescence spectroscopy. Initially, NBHN was dissolved in analytical-grade DMSO to prepare a solution at a concentration of 500 mg/L. Polymers including polyethylene glycol (PEG), polyaspartic acid (PASP), chitosan (CS), polyacrylic acid (PAA), and polyvinyl alcohol (PVA) were individually dissolved in appropriate solvents to yield solutions at a concentration of 1.77×10^{-3} mg/L, which were then mixed with the NBHN solution as components. Then, absorption and fluorescence measurements were conducted in pH 6.0 water using a 1.0 cm quartz cuvette. NBHN probe solution (5 mg/L final concentration) was added, followed by 20 μL of each polymer solution mixed with ultrasound. Then, 20 μL of FA solution (3.5×10^{-3} mg/L) was added, and fluorescence spectra of the five polymer probes were recorded with a 5 nm slit width. The effects of these polymer probes on formaldehyde detection were compared to find an optimal mixed probe solution with high sensitivity and stability.

In the experiments evaluating selectivity, anti-interference capability, quantitative detection, and stability, valuable insights into sensor performance and reliability were derived from tests using a mixed solution of polyacrylic acid and the small molecule formaldehyde probe. These experiments utilized a 35 μM formaldehyde solution prepared from a 37% solution. Various analytes, included

Na^+, Fe^{2+}, Al^{3+}, Co^{2+}, K^+, Mg^{2+}, Cl^-, SO_4^{2-}, Br^-, NO_3^{2-}, glucose, oxidized glutathione, reduced glutathione, H_2O_2, toluene, acetaldehyde, glyoxal, pyruvic aldehyde, sodium pyruvate, salicylaldehyde, and p-nitrobenzaldehyde, were dissolved in distilled water to prepare stock solutions with a concentration of 0.1 mM.

Quantitative detection of formaldehyde

In concentration titration experiments, the concentration of formaldehyde reserve solution (10^{-2} $mol \cdot L^{-1}$) is obtained by diluting formaldehyde (37%) with ultrapure water. Then dilute to different concentrations of formaldehyde solutions (0-200 μM). In fluorescence spectroscopy testing, transfer 2 mL H_2O into a colorimetric dish and add probes PAA and NBHN to obtain a concentration of 17.7 μM PAA@NBHN Probe test solution, then add different concentrations of formaldehyde solution, and observe the fluorescence spectrum after reaction stabilization under test conditions with excitation wavelength of 395 nm and emission spectrum collection range of 415-700 nm.

Colorimetric reagents and test strips for detection

Detection of formaldehyde using fluorescent molecule MBNI and dye crystal violet PAA@NBHN The probe achieved fluorescence color control and developed dual color and tri-color visual colorimetric reagents using a proportional probe strategy. Under the premise of ensuring that the concentration of PAA@NBHN remained constant, the best visual recognition was achieved by repeatedly regulating MBNI with PAA@NBHN = 1:5, gradually going from blue to yellow-green. Crystal violet with PAA@NBHN = 1:2 gradually went from purple to yellow, and in the three-color system MBNI: Cresyl violet: PAA@NBHN = 3:4:3 gradually went from dark purple to light pink. In the paper-based sensor preparation experiments, multiple 1.0×1.0 cm^2 filter papers were soaked in a DMSO-H_2O mixed solution of 1 mM MBNI and PAA@NBHN, dried to obtain paper-based sensors, which were then placed in a sealed formaldehyde environment to visually manifest detection of airborne formaldehyde. In practical applications, samples (including shrimp, mushrooms, and denim fabric) prior to and subsequent to formaldehyde contamination are subjected to heating and vaporization processes to obtain formaldehyde gas. Subsequently, the formaldehyde gas is measured by means of a gas-sampling needle and then introduced into the self-assembled fluorescent test paper. After a reaction period of 10 minutes, the fluorescence variations of the filter

paper under ultraviolet light irradiation are observed, and the RGB values are recorded with the aid of color-recognition software.

Molecular dynamics simulation of PAA@NBHN

Quantum chemistry calculations were performed to optimize the molecular geometries of the compound using Gaussian 16 at the B3LYP/6-311+G(d) level of theory. Bonded and non-bonded interactions within the material structures were described using the OPLS-AA force field,[1] obtained from the AuToFF web server.[2] The PAA chain was composed of 10 monomers, with a mass ratio of PAA to the compound of 7:1. A total of 30 PAA and 15 compound molecules were randomly inserted into a simulation box with dimensions 14.0 nm×14.0 nm×14.0 nm. The steepest descent method minimized the initial energy for each system with a force tolerance of 1 Kj/(mol nm) and a maximum step size of 0.002 ps before MD calculations.[3]

MD simulations were performed using the GROMACS 2021 software package with periodic boundary conditions in all three directions.[4-6] Simulations were conducted in an NVT ensemble for 40 ns, with temperature maintained at 298.15 K using the V-rescale thermostat. Electrostatic interactions were evaluated using Particle-Mesh-Ewald (PME) with fourth-order interpolation, and short-range van der Waals interactions were calculated with a 1.0 nm cutoff.[7] When the distance between the hydrogen atom (H) and the acceptor atom (O) is less than 3.5 Å and the angle formed between the donor atom, the hydrogen atom, and the acceptor atom is larger than 145°, hydrogen bond was considered to be formed. The Independent Gradient Model (IGM) embedded in Multiwfn was employed to analyze weak intermolecular interaction. VMD 1.9.3 was used to render all the images.[8-9]

References

1. W.L. Jorgensen, D.S. Maxwell, J. Tirado-Rives, Development and testing of the opls all-atom force field on conformational energetics and properties of organic liquids. J. Am. Chem. Soc, 1996, 118 (45) , 11225–11236.

2. Wang, C.; Li, W.; Liao, K.; Wang, Z.; Wang, Y.; Gong, K. AuToFF program. Vesrion 1.0. Hzwtech. Shanghai 2023, see https://cloud.hzwtech.com/web/product-service?id=36.

3. Van Gunsteren, W. F.; Berendsen, H., A leap-frog algorithm for stochastic dynamics. Mol. Simul, 1988, 1 (3), 173-185.

4. Spoel D V D, Lindahl E, Hess B, et al. GROMACS: fast, flexible, and free[J]. J. Comput. Chem, 2005, 26(16), 1701-1718.

5. Abraham, et al. GROMACS: high performance molecular simulations through multi-level parallelism from laptops to supercomputers, SoftwareX. 2015, 1, 19–25.

6. H.J.C. Berendsen, D. van der Spoel, R. van Drunen,GROMACS: A message-passing parallel molecular dynamics implementation,Comp. Phys. Comm, 1995, 91, 43-56.

7. Darden T, York D, Pedersen L. Particle Mesh Ewald: An nlog (N) method for ewald sums in large systems [J]. J. Chem. Phys, 1993, 98(12), 10089-10092.

8. Humphrey, W.; Dalke, A.; Schulten, K., VMD: Visual molecular dynamics. J. Mol. Graph. 1996, 14, 33-38.

9. Gaussian 16, Revision C.01, M. J. Frisch, G. W. Trucks, H. B. Schlegel, G. E. Scuseria, M. A. Robb, J. R. Cheeseman, G. Scalmani, V. Barone, G. A. Petersson, H. Nakatsuji, X. Li, M. Caricato, A. V. Marenich, J. Bloino, B. G. Janesko, R. Gomperts, B. Mennucci, H. P. Hratchian, J. V. Ortiz, A. F. Izmaylov, J. L. Sonnenberg, D. Williams-Young, F. Ding, F. Lipparini, F. Egidi, J. Goings, B. Peng, A. Petrone, T. Henderson, D. Ranasinghe, V. G. Zakrzewski, J. Gao, N. Rega, G. Zheng, W. Liang, M. Hada, M. Ehara, K. Toyota, R. Fukuda, J. Hasegawa, M. Ishida, T. Nakajima, Y. Honda, O. Kitao, H. Nakai, T. Vreven, K. Throssell, J. A. Montgomery, Jr., J. E. Peralta, F. Ogliaro, M. J. Bearpark, J. J. Heyd, E. N. Brothers, K. N. Kudin, V. N. Staroverov, T. A. Keith, R. Kobayashi, J. Normand, K. Raghavachari, A. P. Rendell, J. C. Burant, S. S. Iyengar, J. Tomasi, M. Cossi, J. M. Millam, M. Klene, C. Adamo, R. Cammi, J. W. Ochterski, R. L. Martin, K. Morokuma, O. Farkas, J. B. Foresman, and D. J. Fox, Gaussian, Inc., Wallingford CT, 2019.

2. Supporting figures

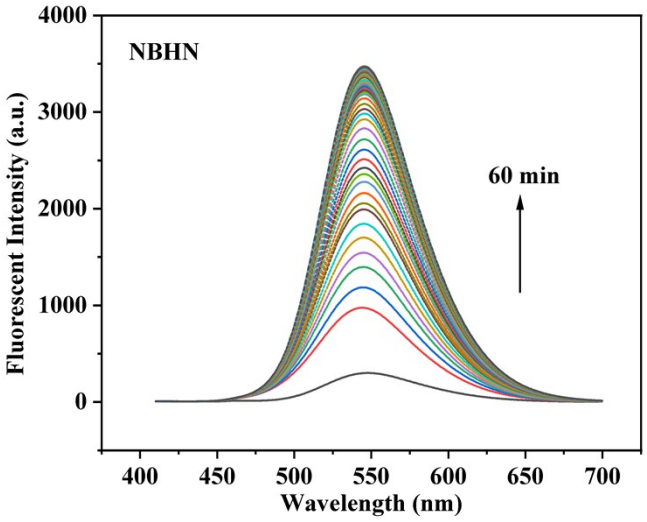

Fig. S1. Time-dependent fluorescence spectra of NBHN aqueous solution with the addition of FA.

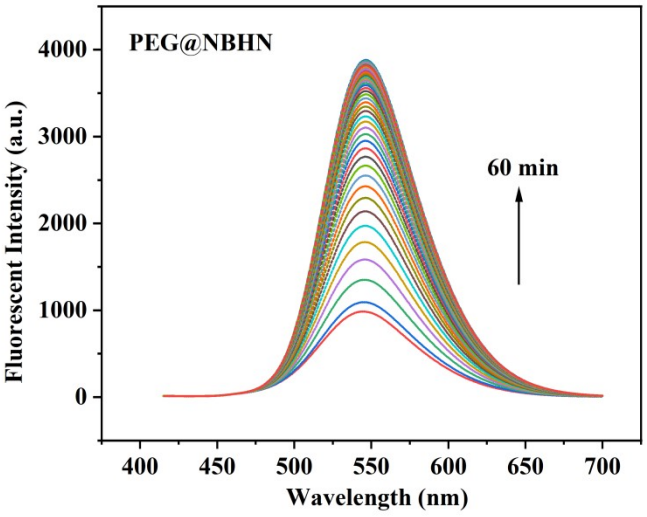

Fig. S2. Time-dependent fluorescence spectra of PEG@NBHN aqueous solution with the addition of FA.

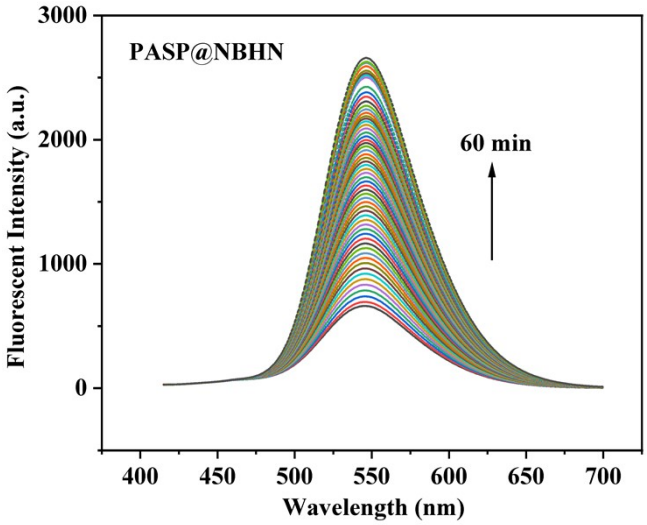

Fig. S3. Time-dependent fluorescence spectra of PASP@NBHN aqueous solution with the addition of FA.

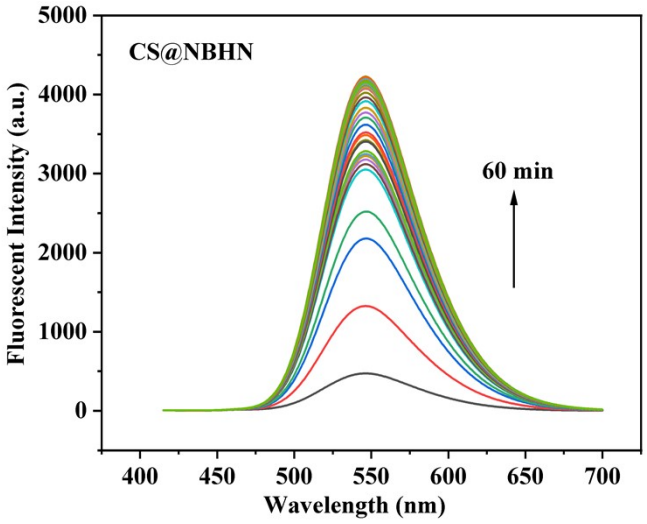

Fig. S4. Time-dependent fluorescence spectra of CS@NBHN aqueous solution with the addition of FA.

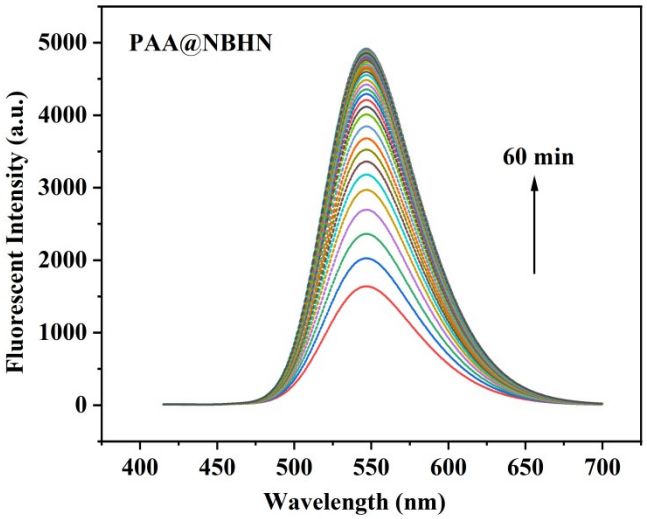

Fig. S5. Time-dependent fluorescence spectra of PAA@NBHN aqueous solution with the addition of FA.

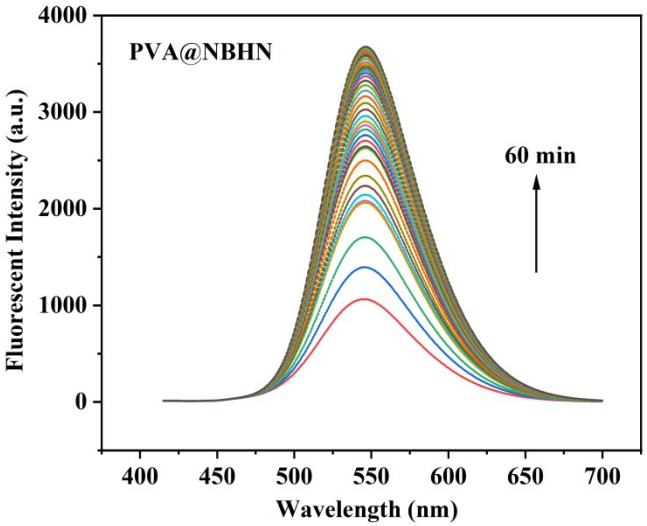

Fig. S6. Time-dependent fluorescence spectra of PVA@NBHN aqueous solution with the addition of FA.

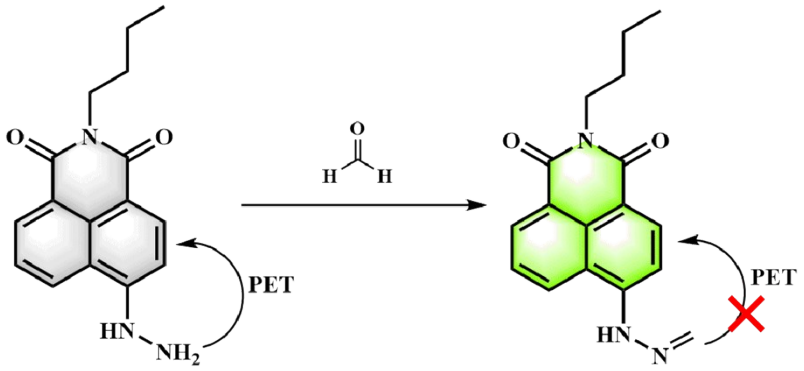

Fig. S7. Schematic illustration of the reaction mechanism of the small molecule formaldehyde fluorescent probe NBHN with FA.

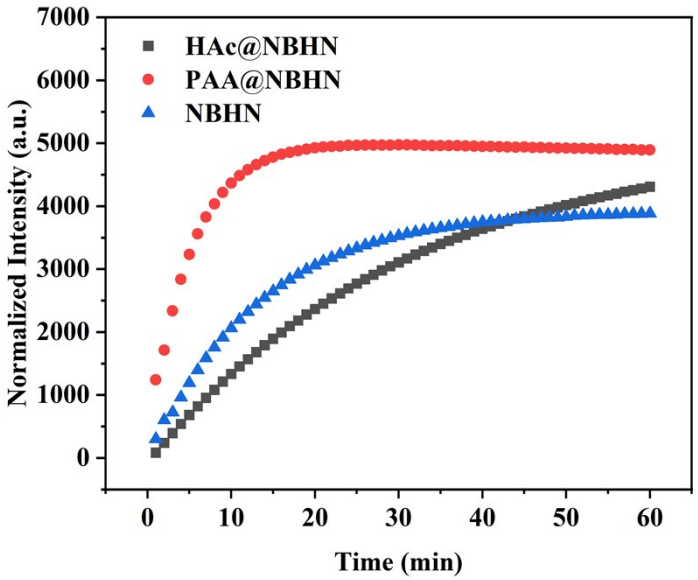

Fig. S8. Fluorescence intensity alterations at 545 nm for probe NBHN, HAc@NBHN, and PAA@NBHN (final value, 17.7 μM) in response to FA (35 μM) within the aqueous solution.

Fig. S9. Fluorescence images of PAA and NBHN aqueous solutions upon the addition of FA under 365 nm UV light.

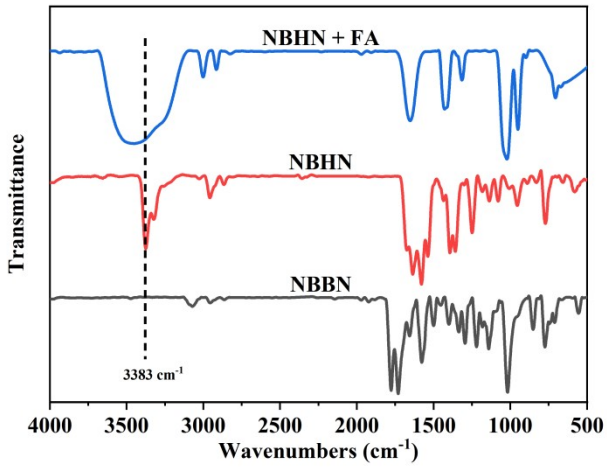

Fig. S10. FT-IR spectra of NBBN, NBHN and NBHN + FA solutions.

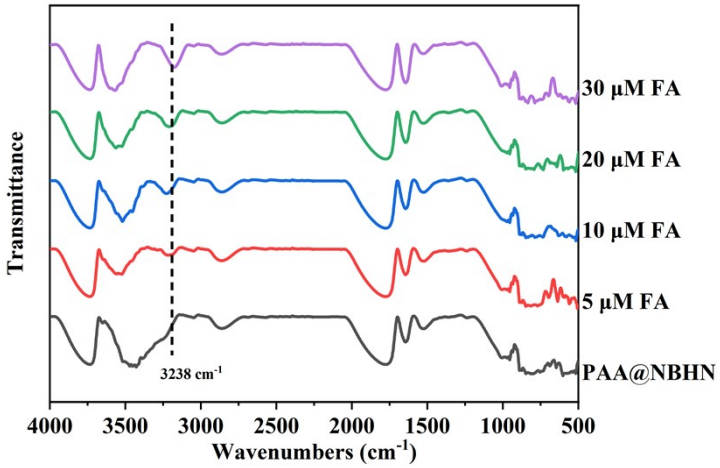

Fig. S11. FT-IR spectra of PAA@NBHN solution after the addition of different concentrations of FA.

		Size (d.nm):	% Number:	St Dev (d.nm):
Z-Average (d.nm): 279.7	Peak 1:	59.69	100.0	25.17
PdI: 0.440	Peak 2:	0.000	0.0	0.000
Intercept: 0.956	Peak 3:	0.000	0.0	0.000

Result quality : Good

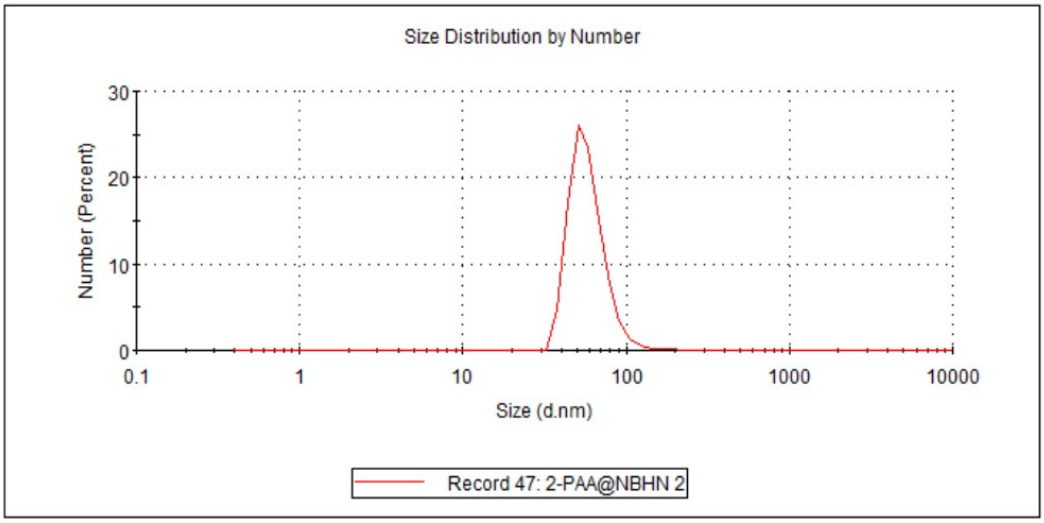

Fig. S12. Dynamic light scattering (DLS) analysis of PAA@NBHN solution.

		Size (d.nm):	% Number:	St Dev (d.nm):
Z-Average (d.nm): 209.7	Peak 1:	70.47	100.0	32.92
PdI: 0.231	Peak 2:	0.000	0.0	0.000
Intercept: 0.961	Peak 3:	0.000	0.0	0.000

Result quality : Good

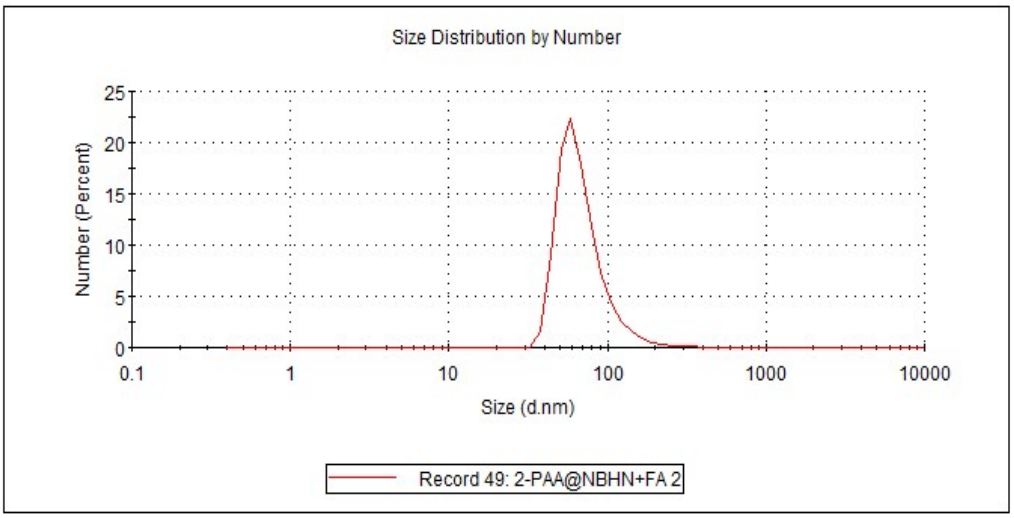

Fig. S13. DLS analysis of the PAA@NBHN solution after reaction with FA.

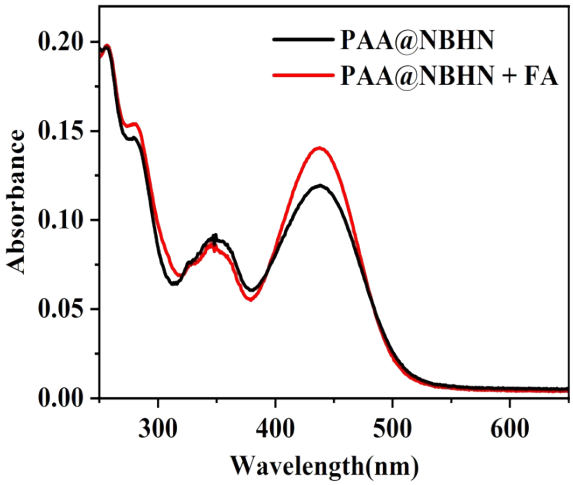

Fig. S14. Absorption spectra of PAA@NBHN before and after reaction with FA (35 μM).

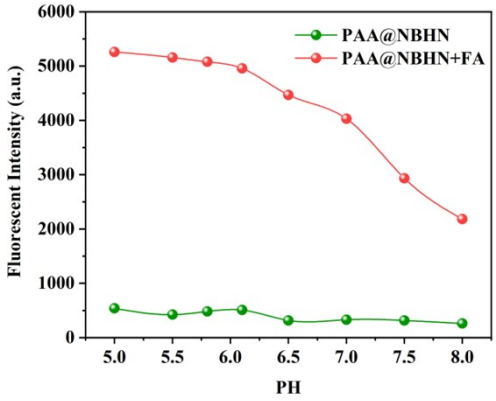

Fig. S15. Fluorescence intensity at 545 nm of PAA@NBHN, pre- and post-interaction with FA, across a pH range of 5 to 8.

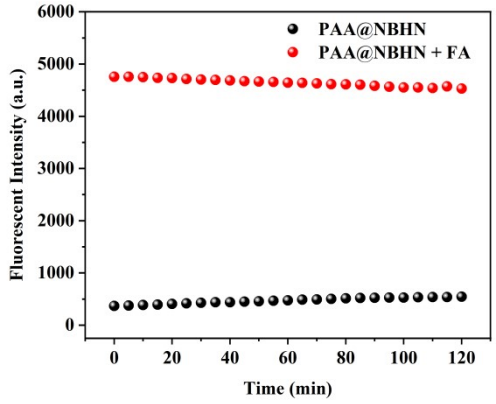

Fig. S16. Changes in fluorescence intensity at 545 nm of PAA@NBHN and its reaction product with FA under light exposure over a 2-hour timescale.

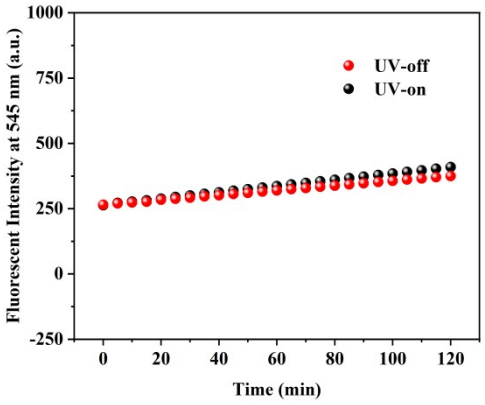

Fig. S17. Photostability profiles of the free probe NBHN under conditions with and without 395 nm UV irradiation.

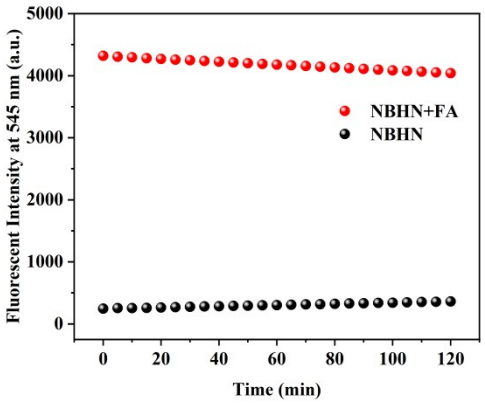

Fig. S18. Photostability profiles of probe NBHN before and after response to FA under 395 nm UV irradiation.

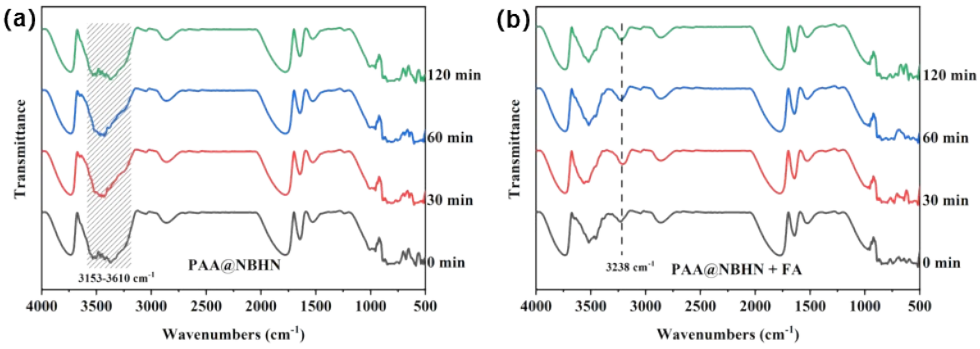

Fig. S19. FT-IR spectra of PAA@NBHN(a) and PAA@NBHN+FA(b) at various time intervals.

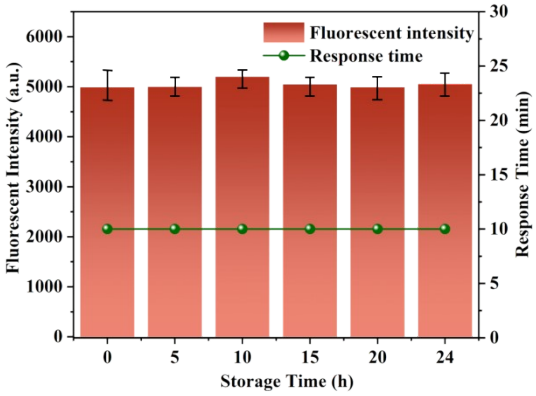

Fig. S20. Fluorescence response of the probe PAA@NBHN to FA (35 μM) at various storage durations.

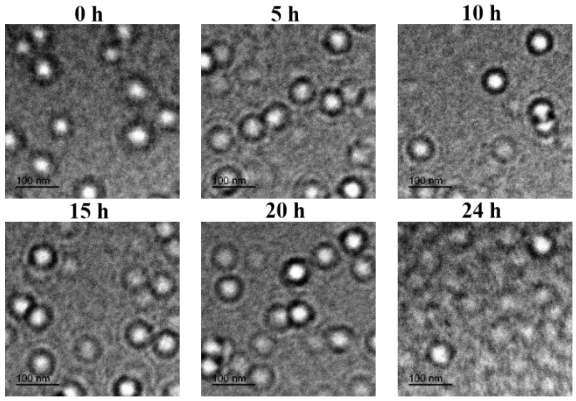

Fig. S21. TEM images of probe PAA@NBHN at different storage times.

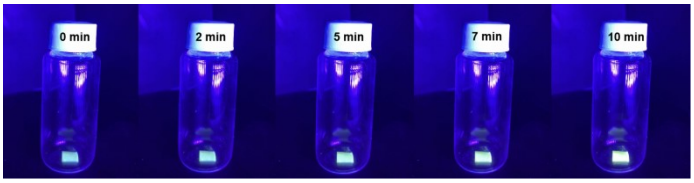

Fig. S22. Time response images of the test paper to FA in contaminated samples (denim fabric) under UV lamp irradiation.

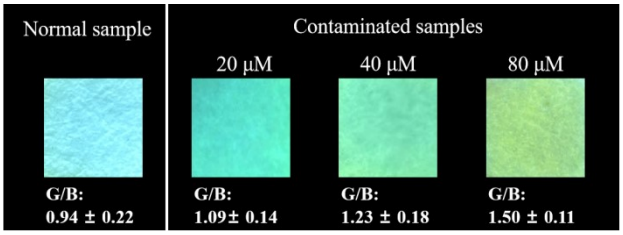

Fig. S23. Fluorescence color of the test paper in samples (denim fabric) with different concentrations of FA pollution under UV lamp irradiation.

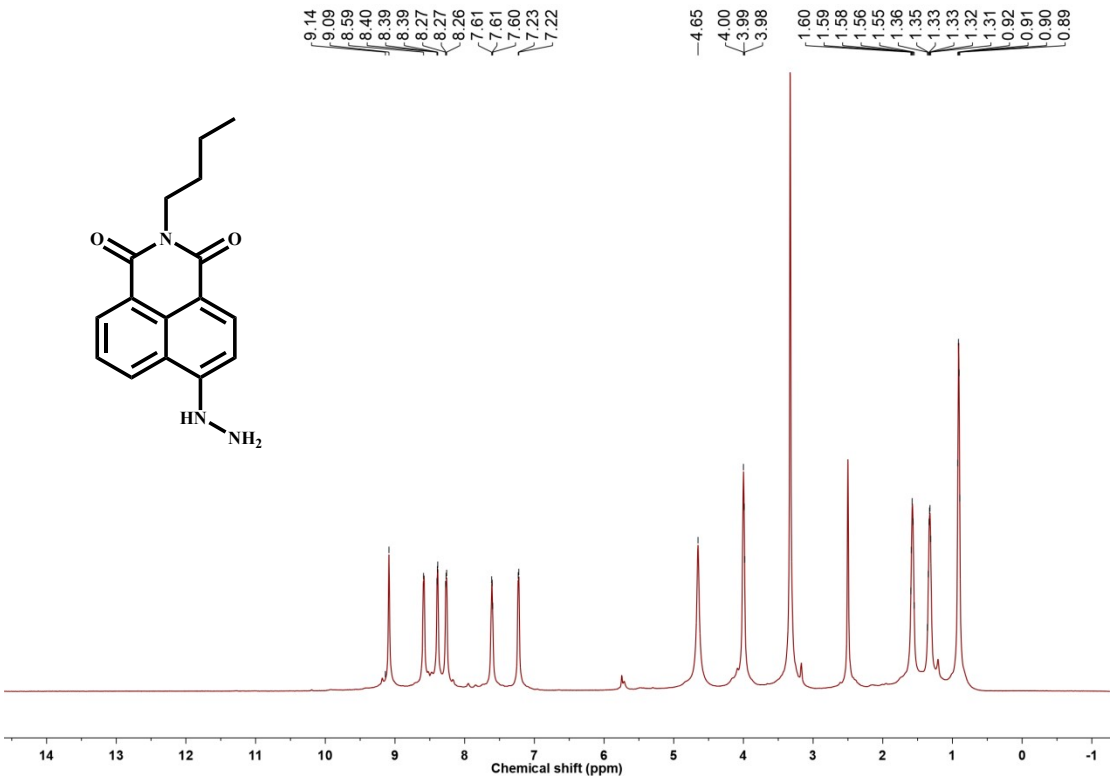

Fig. S24. ^{1}H NMR (DMSO, 600 MHz) spectrum of NBHN.

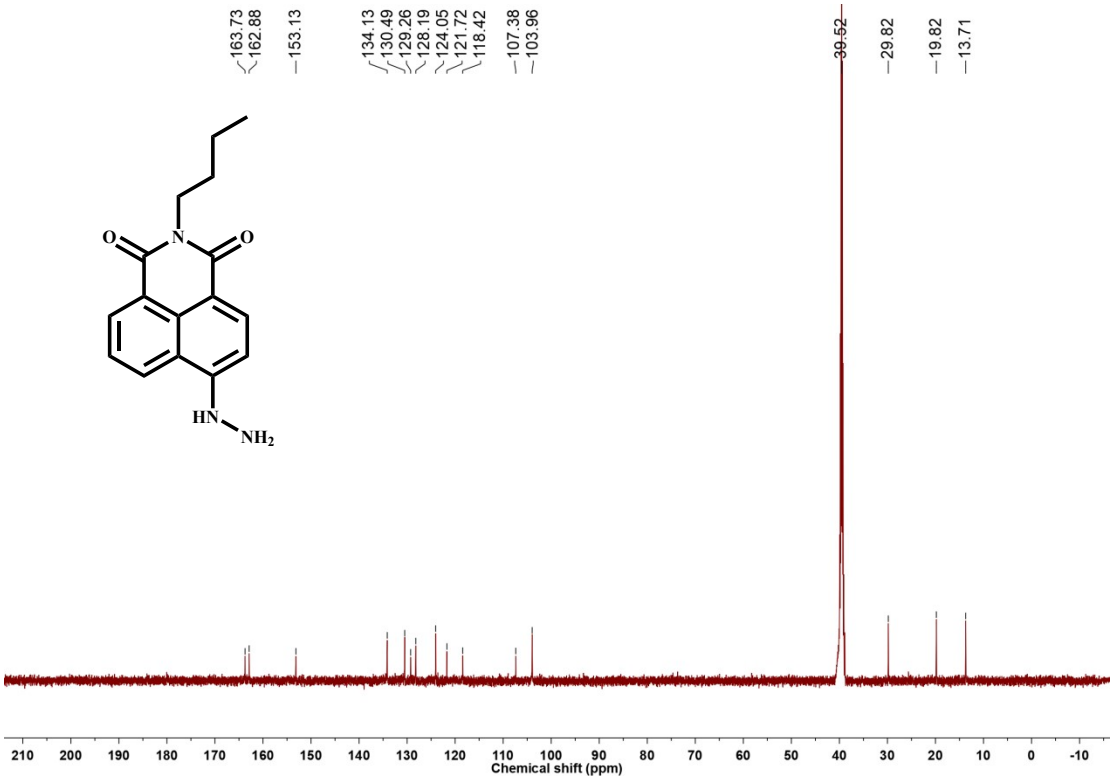

Fig. S25. ^{13}C NMR (DMSO, 151 MHz) spectrum of NBHN.

3. Supporting Tables

Table S1. Comparison of the performance of different FA probes in terms of their response .

Reference	Probe	Detection limit	Detection time
Angew. Chem. Int. Ed, 2016, 55, 3356-3359.	Na-FA	0.71 μM	30 min
ACS. Appl. Bio. Mater, 2019, 2(1), 555-561.	P-FA	6.1 μM	90 min
Food. Chemistry, 2022, 384, 132426-132426.	Probe-NH_2	1.87 μM	30 min
Food. Chemistry, 2023, 411, 135483	NFD	0.95 μM	30 min
This work	PAA@NBHN	0.94 μM	10 min

Table S2. Costs of the probe PAA@NBHN.

Chemicals	Dosage[a]	Unit price (CNY/g)	Total
H_2O	200%	$5*10^{-6}$	**0.18057 CNY**
4-Br-1,8-Naphthalenedioic Anhydride	0.5%	30.2	
Butylamine	0.148%	0.23	
Hydrazine Hydrate	0.2%	2	
Ethanol	3%	0.006	
PAA	0 .007%	72	
DMSO	2%	1	

Note: [a]Based on the content of a single detection reagents.